Archives of Photogrammetry, Cartography and Remote Sensing, Vol. 22, 2011, pp. 437-449
ISSN 2083-2214

STOCHASTIC MODELLING AND ANALYSIS OF IMU SENSOR ERRORS

Yueming Zhao [1], Milan Horemuz [2], Lars E. Sjöberg [3]

[1, 2, 3] Division of Geodesy and Geoinformatics, Royal Institute of Technology (KTH),
SE-100 44 Stockholm, Sweden
(yueming, horemuz, lsjo)@kth.se

KEY WORDS: IMU, integration, sensor, random, accuracy, navigation

ABSTRACT The performance of a GPS/INS integration system is greatly determined by the ability of stand-alone INS system to determine position and attitude within GPS outage. The positional and attitude precision degrades rapidly during GPS outage due to INS sensor errors. With advantages of low price and volume, the Micro Electrical Mechanical Sensors (MEMS) have been wildly used in GPS/INS integration. Moreover, standalone MEMS can keep a reasonable positional precision only a few seconds due to systematic and random sensor errors. General stochastic error sources existing in inertial sensors can be modelled as (IEEE STD 647, 2006) Quantization Noise, Random Walk, Bias Instability, Rate Random Walk and Rate Ramp. Here we apply different methods to analyze the stochastic sensor errors, i.e. autoregressive modelling, Gauss-Markov process, Power Spectral Density and Allan Variance. Then the tests on a MEMS based inertial measurement unit were carried out with these methods. The results show that different methods give similar estimates of stochastic error model parameters. These values can be used further in the Kalman filter for better navigation accuracy and in the Doppler frequency estimate for faster acquisition after GPS signal outage.

1. INTRODUCTION

For a long time the Inertial Measurement Units (IMU) used in navigation systems were heavy and expensive. Then gradually the Micro Electrical Mechanical Sensor (MEMS) with great advantages of price and volume is widely used in GPS/INS integrated systems. Although the accuracy of MEMS is improved rapidly during latest years, the MEMS stand-alone navigation during GPS signal blockage could still only maintain a reasonable error within a very short time due to the integration of sensor errors.

The systemic errors (i.e. bias and scale errors) of MEMS must be estimated before navigation sessions. According to IEEE STD 647, 2006, we verify different stochastic analysis methods to estimate the noise model parameters, i.e. Quantization Noise, Random Walk, Bias Instability, Rate Random Walk and Rate Ramp.

In this paper several stochastic analysis methods are introduced, including autoregressive (AR) modelling, Gauss-Markov (GM) process, Power Spectral Density (PSD) and Allan Variance (AV). Tests on a MEMS based IMU are carried out with these methods.

2. METHODOLOGY OF MEMS ERROR MODELING

2.1 Autoregressive model

An m-variate p-order autogressive (AR(p)) model for a stationary time series of state vectors $\mathbf{v}_v$, observed at equally spaced instants v, is defined by (Neumaier and Schneider, 2001)

$$\mathbf{v}_v = \mathbf{w} + \sum_{l=1}^{p} \mathbf{A}_l \mathbf{v}_{v-l} + \boldsymbol{\varepsilon}_v \tag{1}$$

or

$$\mathbf{v}_v = \mathbf{B}\mathbf{u}_v + \boldsymbol{\varepsilon}_v \tag{2}$$

where $\boldsymbol{\varepsilon}_v$ are uncorrelated random vectors with zero mean and covariance matrix $\mathbf{C}$, $\mathbf{A}_l$ are the coefficient matrices of the AR model, $\mathbf{w}$ is a vector of intercept terms to allow for a nonzero mean of the time series and $\mathbf{B} = (\mathbf{w} \quad \mathbf{A}_1 \quad \ldots \quad \mathbf{A}_p)$, $\mathbf{u}_v^T = (1 \quad \mathbf{v}^T{}_{v-1} \quad \ldots \quad \mathbf{v}^T{}_{v-p})$. From Eq. (1) we can see that the current sample $\mathbf{v}_v$ can be estimated by the previous p samples. The one-variate AR(1) and AR(2) models in discrete time are

$$x_k = \phi_1 x_{k-1} + w_k \tag{3a}$$

$$x_k = \phi_1 x_{k-1} + \phi_2 x_{k-2} + w_k \tag{3b}$$

where x is the random variable, subscript k is the discrete time index, $\phi_{1,2}$ are the coefficients to be estimated and w_k is zero-mean Gaussian white noise with variance $\sigma_{w_k}^2$.

To use the AR model we should first fix its order and then the value of each coefficient. There are several methods to determine the order of the AR model. Here we use Schwarz's Bayesian Criterion (SBC; Schwarz, 1978; Neumaier and Schneider, 2001), which states that the AR order p should minimize the criterion

$$SBC(p) = \frac{l_p}{m} - (1 - \frac{n_p}{N}) \log N = \min_p . \tag{4}$$

where $l_p = \log(\det \boldsymbol{\Delta}_p)$, $\boldsymbol{\Delta}_p$ is the residual cross-product matrix and N is the number of samples, m is the dimension of the state vector, and $n_p = mp + 1$ is the dimension of $\mathbf{v}_v$. For Eq. (3), $m=1$.

The AR model parameters can be estimated using least-squares fitting, Yule-Walker equations (Eshel, 2010) or Burg's method (Bos et al., 2002). A stepwise least-squares algorithm is used in this paper after the order has been fixed (Neumaier and Schneider, 2001; Zhao, 2011). By means of the moment matrices

$$\mathbf{U} = \sum_{v=1}^{N} \mathbf{u}_v \mathbf{u}_v^T, \mathbf{V} = \sum_{v=1}^{N} \mathbf{v}_v \mathbf{v}_v^T, \mathbf{W} = \sum_{v=1}^{N} \mathbf{v}_v \mathbf{u}_v^T \tag{5}$$

the least-squares estimates of the parameter matrix and the residual covariance matrix in Eq. (2) can be written as

$$\hat{\mathbf{B}} = \mathbf{W}\mathbf{U}^{-1} \tag{6}$$

$$\hat{\mathbf{C}} = \frac{1}{N - n_p}(\mathbf{V} - \mathbf{W}\mathbf{U}^{-1}\mathbf{W}^{\mathrm{T}}) \tag{7}$$

The variance of estimation noise can be given as

$$\sigma_{w_k}^2 = \frac{1}{n}\sum_{i=1}^{n}(x_i^d - \hat{x}_i)^2 \tag{8}$$

where n is the size of the sample of the stationary process, x_i^d is the known value of the process (desired output), and $\hat{x}_i$ is the corresponding estimated output.

2.2 Gauss-Markov process

The Gauss-Markov (GM) processes are stationary processes that have exponential Auto Correlation Functions (ACF). The first-order GM process is frequently used to describe a correlated signal, which is defined by the exponential ACF:

$$R_x(\tau) = \sigma^2 e^{-\beta|\tau|} \tag{9}$$

where σ^2 is the noise variance, β^{-1} is the correlation time and τ is the time interval. The ACF of Eq. (9) is shown in Figure 1. From this figure we can see that there is a peak at zero, and there are two symmetrical descendent slopes at both sides, and the gradient at zero is discontinuous. For the second- and third-order GM process models, we refer to Gelb, 1974.

The first-order GM process in discrete time and the variance are given as

$$x_k = e^{-\beta\Delta t}x_{k-1} + w_k \tag{10}$$

$$\sigma_{x_k}^2 = \sigma_{w_k}^2 / (1 - e^{-2\beta\Delta t_k}) \tag{11}$$

where Δt is the discrete time sampling interval.
From equations (3) and (9), we obtain

$$e^{-\beta\Delta t} = \phi_1 \tag{12}$$

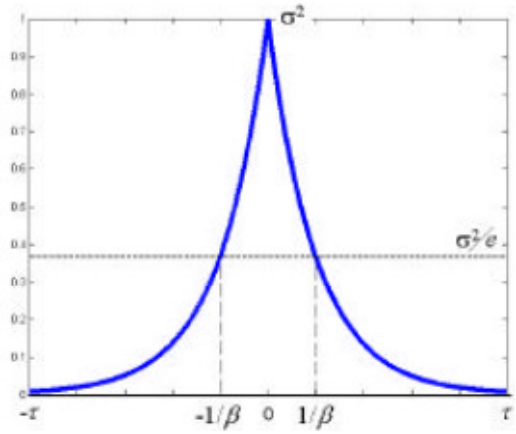

Fig. 1. ACF of GM process

Therefore, the relation between the two models can be shown as

$$\beta = -\ln \phi_1 / \Delta t \tag{13}$$

However, the principle difference between the AR model and the GM process should be declared. The AR model does not consider the sampling interval, which may be considered as a sub-optimal estimation of the noise process. The GM-only model needs a long data set, for example 200 times of the expected correlation time for 10% uncertainty of the estimated noise model parameters (Nassar, 2005).

2.3 Power Spectral Density

The Power Spectral Density (PSD) is a commonly used and powerful tool for analyzing a signal or time series. In statistical signal processing, the PSD describes the distribution of energy in frequency domain. For a finite-energy signal $f(t)$, the definition of PSD is

$$S(\omega) = \left| \frac{1}{\sqrt{2\pi}} \int_{-\infty}^{+\infty} f(t) e^{-i\omega t} dt \right|^2 = \frac{F(\omega) F^*(\omega)}{2\pi} \tag{14}$$

where ω is the frequency, $F(\omega)$ and $F^*(\omega)$ are the Fourier transform of $f(t)$ and its complex conjugate respectively. A key point is that the two-sided PSD $S(\omega)$ and autocorrelation function $K(\tau)$ are Fourier transform pairs, if the signal can be treated as a wide-sense stationary random process (IEEE Std. 952, 1997):

$$S(\omega) = \int_{-\infty}^{+\infty} e^{-j\omega\tau} K(\tau) d\tau \tag{15}$$

$$K(\tau) = \frac{1}{2\pi} \int_{-\infty}^{+\infty} e^{j\omega\tau} S(\omega) d\omega \tag{16}$$

This relation also provides an approach to compute the PSD.

The typical characteristic slopes of the PSD for sensor errors can be found in (IEEE Std. 952, 1997; Hou, 2004). With real data, gradual transitions would exist between the different PSD slopes (IEEE Std. 1293, 1998), rather than the sharp transitions, and the slopes might be different from the typical values.

2.4 Allan Variance

The Allan Variance (AV) is a method of representing root mean square (RMS) random drift error as a function of averaging time (Allan, 1966). As a time domain analysis technique, it is an accepted IEEE standard for gyro specifications (IEEE Std. 647, 2006). If there are *N* samples of data points with sampling interval Δt , then a group of *n* data points with $n < (N-1)/2$ can be created. Each group is called a cluster $\tau = n\Delta t$. Assume that the instantaneous sample of the sensor is the angular velocity $\Omega(t)$, and its integration is the angle:

$$\theta(t) = \int^{t} \Omega(t')dt' \tag{17}$$

The average angular velocity in the k-th cluster, i.e. between time interval t_k and $t_k + \tau$, is

$$\overline{\Omega}_k(\tau) = \frac{1}{\tau} \int_{t_k}^{t_k+\tau} \Omega(t)dt \tag{18}$$

and the AV is defined as

$$\begin{aligned} \sigma^2 &= \frac{1}{2}\left\langle (\overline{\Omega}_{k+n} - \overline{\Omega}_k)^2 \right\rangle \\ &= \frac{1}{2\tau^2}\left\langle (\theta_{k+2n} - 2\theta_{k+n} + \theta_k)^2 \right\rangle \end{aligned} \tag{19}$$

where the symbol < > is the infinite time average. In practice, the AV can be estimated with a finite number of samples by the so-called overlapped AV, which has been accepted as the preferred AV estimator in many standards:

$$\begin{aligned} \sigma^2 &\approx \frac{1}{2(N-2n)} \sum_{k=1}^{N-2n} (\overline{\Omega}_{k+1}(T) - \overline{\Omega}_k(T))^2 \\ &= \frac{1}{2\tau^2(N-2n)} \sum_{k=1}^{N-2n} (\theta_{k+2n} - 2\theta_{k+n} + \theta_k)^2 \end{aligned} \tag{20}$$

There is a unique relation between the AV and the PSD of a stationary process (IEEE Std.952, 1997)

$$\sigma^2(\tau) = 4\int_0^{+\infty} S(\omega)\frac{\sin^4(\pi\omega\tau)}{(\pi\omega\tau)^2}d\omega \tag{21}$$

Table 1 shows the relation between curve slope and coefficient values on the log-log figure of the AV (For the detailed derivation, we refer to Hou, 2004). The AV of the total stochastic process can be assumed as the sum of all different error terms, since they are independent on different time regions. The total AV of the system can then be expressed as:

$$\sigma_{tot}^2 = \sigma_{quant}^2 + \sigma_{RW}^2 + \sigma_{Bias}^2 + \sigma_{BRW}^2 + ... \tag{22}$$

Standard Allan Variance is also named Allan Deviation (AD). From the AD plot, it is straightforward to identify various random processes that exist in the raw data and get the noise coefficients from Table 1.

Tab. 1. Summary of characteristic curve slope and coefficient value (Zhang et al., 2008)

Error Type	Curve slope	Coefficient value
Quantisation Noise	-1	$Q = \sigma(\sqrt{3})$
Random Walk	-1/2	$N = \sigma(1)$
Bias Instability	0	$B = \frac{\sigma(f_0)}{0.664}$
Rate random walk	+1/2	$K = \sigma(3)$
Rate ramp	+1	$K = \sigma(\sqrt{2})$
Correlated Noise	±1/2	$q_c T_c = \sigma(1)$ $q_c = \sigma(3)$

A typical AV plot is shown in Figure 2. For example, it is well known that the random walk is a significant noise component in low cost inertial sensors. The angular random walk coefficient with unit deg/h$^{1/2}$ can be identified at T=1 h with a straight line of slope -1/2 as shown in Figure 2.

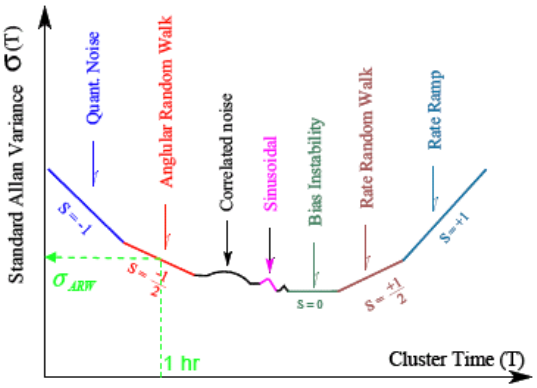

Fig. 2. Allan variance analysis noise terms results (IEEE Std. 952-1995, 1998)

In practice, the AV is based on a finite number of independent clusters that can be formed from any finite length of data. The AV of any noise term is estimated using the total number of clusters of a given length that can be created. The confidence of the estimation improves as the number of independent clusters is increased. For *n* points in each cluster, a straightforward percentage error calculation for the estimated coefficients as listed in Table 1 is given as (Barnes et al.,1971; El-Sheimy et al., 2008)

$$\sigma = [2(\frac{N}{n} - 1)]^{-1/2} \times 100\% \tag{23}$$

3. TEST RESULTS

The testing platform is based on ISIS-IMU from Inertial Science Inc., a six-degree of freedom inertial measurement unit designed for commercial use as shown in Figure 3. The following test results are all based on 2 hour static data from the ISIS-IMU.

Fig. 3. ISIS-IMU

Since there are 3 gyros and 3 accelerometers in the IMU, there would be $p \times 6$ parameters and 6 noise variances if the model is fixed to p-th order for all 6 sensors. In the real test, we found that the order of AR model that minimize the SBC would vary with different length of data samples as well as different sensors, while the residual variance matrix would just change a little. Therefore, we can determine that a second-order AR (2) model can be applied for all gyros and accelerometers. The ARM_{FIT}^{TM} package (Schneider and Neumaier, 2001) is used to estimate the AR model parameters. One way to check whether the estimated order is valid is to verify the whiteness of the model residuals. From Figure 4 we can see that the residuals of AR (2) for the accelerometer along y-axis are nearly white noise (within 95% confidence interval between two horizontal lines).

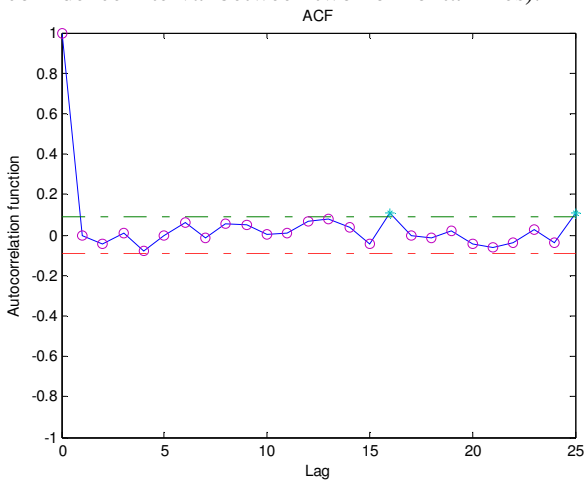

Fig. 4. ACF of AR(2) residual for Y-Accelerometer

From the collected static data, we can get the PSD plot of the gyro along x-axis as shown in Figure 5. A certain amount of noise would exist in the plotted curve due to the uncertainty.

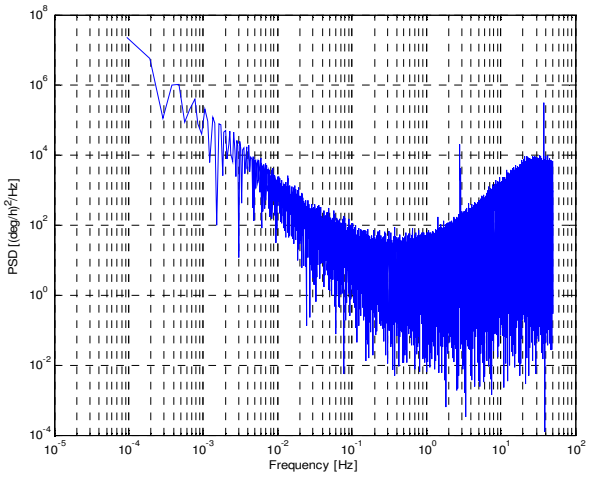

Fig. 5. X-Gyro PSD

The bunching and flickers in high frequency of the PSD plot prevent us from further analysis. The frequency averaging technique (IEEE Std.1293, 1998) is used to average the points among the high frequencies of the PSD result in Figure 6.

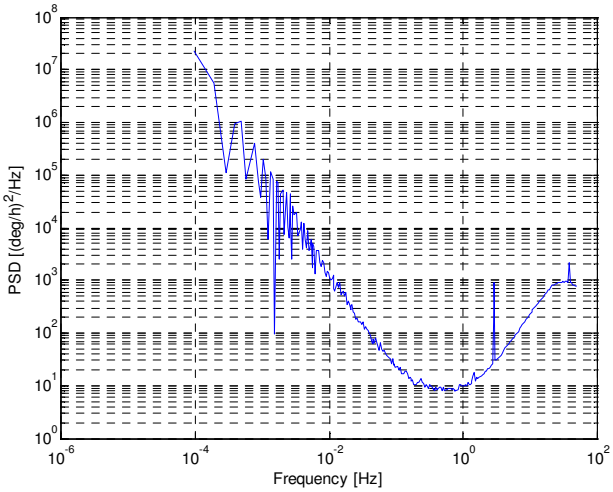

Fig. 6. X-Gyro PSD after frequency averaging

The slopes of the PSD curve include –2, 0, and +2, which indicate that the X-axis gyro data contains rate random walk, random walk, and quantization noise, respectively. The acquisition of parameters for noise terms from the PSD result plot is complex. Applying the random walk parameter equation (IEEE Std. 952, 1997)

$$Q(^0/\sqrt{h}) = \frac{1}{60}\sqrt{\frac{1}{2}PSD[(^0/\sqrt{h})^2 / Hz]} \tag{24}$$

we obtain a random walk parameter of about 0.024 deg/h^{½}. According to the specification, the random walk parameter is less than 0.5 deg/h^{½}. The reason why the experiment result is much smaller may be that these experiments are carried out during static situations, while in dynamic situations it may go up.

The AD plot for gyros and accelerometers are shown in Figure 7 and Figure 9, respectively. The standard error of each AD can be evaluated with Eq. (23) as shown in Figure 8. With these two figures, we can identify different error coefficients by means of Table 1 as listed in Table 2 and Table 3 for gyros and accelerometers, respectively. For instance, the quantization noise coefficient can be obtained by the value of the straight fitting line from the beginning with slope -1 at the time T= $\sqrt{3}$ h. The reason for the big quantization noise for accelerometer Z may be that the specific force sensed by the accelerometer along the vertical direction is overwhelmingly influenced by the gravity.

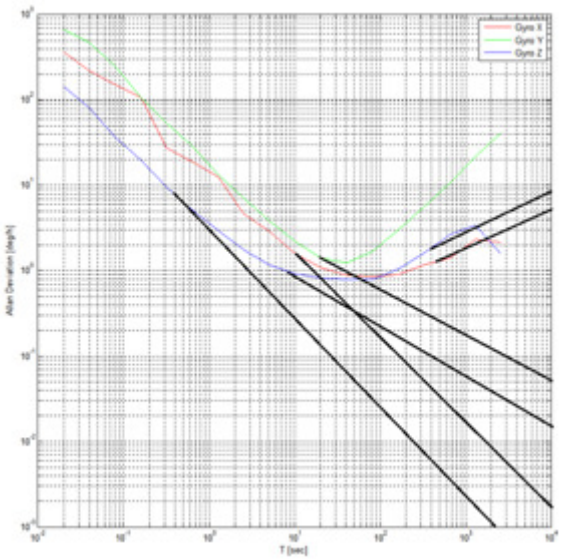

Fig. 7. AD plot for 3 gyros with fitting lines

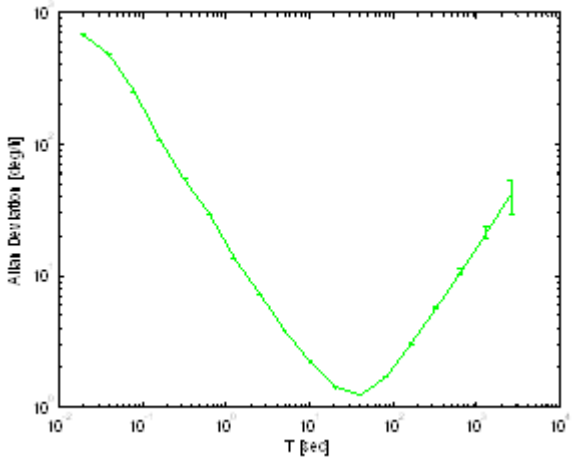

Fig. 8. AD plot for Y-Gyro with percentage errors (I bar)

Tab. 2. Error coefficients for gyros

	Gyros X	Gyros Y	Gyros Z
Quantisation noise (deg)	2.5×10^{-3}	7.2×10^{-3}	9.1×10^{-4}
Random walk (deg/h$^{1/2}$)	4.8×10^{-2}	N/A	2.6×10^{-2}
Bias instability (deg/h)	1.4	N/A	1.2
Rate random walk (deg/h$^{3/2}$)	5.2	N/A	8.1
Rate ramp (deg/h^2)	N/A	72	N/A

Please note that the quantization error defined in IEEE standards, which are referred in this paper, is actually a kind of bit quantization error caused by the transformation from analogue value to digital value for the MEMS sensor measurements. However, there is another kind of time quantization error caused by synchronization error of the sampling pulse. For more detailed information on time quantization errors, we refer to Savage, 2002.

Tab. 3. Error coefficients for accelerometers (Acc.)

	Acc. X	Acc. Y	Acc. Z
Quantisation noise (m/s)	4.5×10^{-3}	2.1×10^{-3}	4.8×10^{-1}
Bias instability (m/s^2)	1.4	0.9	N/A
Rate ramp ($m/s/h^2$)	N/A	3.2	N/A

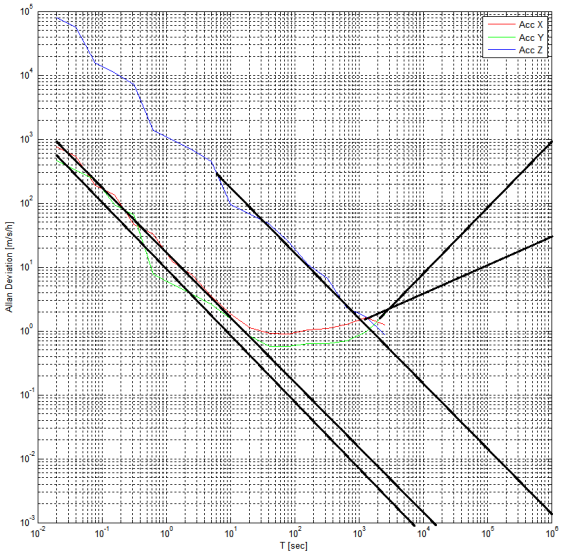

Fig. 9. AD plot for 3 accelerometers with fitting lines

4. DISCUSSION AND CONCLUSION

Using different models, we analyzed the sensor errors and got the parameters. We can use the AR model to estimate next consecutive errors, if we do not care much about different error components themselves and treat them totally together as stochastic errors. Although the optimal AR model would change its order with different sensors, a second-order AR model can be accepted as the unique model for all sensors of the IMU. Since the first-order GM process can be treated as a first-order AR model, if the sample interval is fixed, we do not specifically analyse this most commonly used model.

The PSD is also a common tool to analyze both periodic and non-periodic signals. Frequency averaging is needed to get the exact slopes of the curve, but the parameters are difficult to compute directly. Also it may be somewhat difficult for the non-system analyst to understand, since it is in the frequency domain.

AV analysis has been widely used for MEMS stochastic modelling, due to its simplicity and effectiveness. It is a great advantage that the noise terms differ from region to region. And there is a relation between the AV and the PSD. Therefore, different noise coefficients can be easily obtained with the AV plot. However, a long static data record may be required, even dozens of hours, as we can see that the long-time slope is sometimes not fully determined within several hours of data.

Although different methods may give different values of the noise coefficients, similar noise sources can be verified with a specific sensor. It is expected that with longer data sets and many iterations a set of more accurate coefficients can be estimated. After getting the coefficients for the main stochastic errors, a better error model can be applied in the GPS/INS integrated system, which is of much help for the Doppler frequency estimate and for bounding the error drift during GPS outage.

REFERENCES:

Allan D. W., 1966. Statistics of atomic frequency standards, *Proceedings of the IEEE*, 54(2), pp. 221–230.

Barnes J. A. et al.,1971. Characterization of frequency stability. *IEEE Trans. Instrum. Meas*., vol. IM-20, no. 2, pp. 105–120.

Bos R., Waele S. D. & Broersen P. M. T., 2002. Autoregressive spectral estimation by application of the Burg algorithm to irregularly sampled data. *IEEE Trans. on Instrumentation and Measurement*, 51(6), pp. 1289-1294.

Eshel G., 2010. The Yule Walker Equations for the AR Coefficients. University of South Carolina.
http://www.stat.sc.edu/~vesselin/STAT520_YW.pdf.

Gelb A., 1974. Applied Optimal Estimation. MIT Press. Cambridge, Massachusetts.

Hou H., 2004. Modeling inertial sensors errors using AV, M.S. thesis, MMSS Res. Group, Dept. Geomatics Eng., Univ. Calgary. Canada.
http://www.ucalgary.ca/engo_webdocs/ NES/04.20201. HaiyingHou.pdf

IEEE Std. 1293, 1998. IEEE Standard Specification Format Guide and Test Procedure for Linear, Single-Axis, Non-gyroscopic Accelerometers.

IEEE Std. 952, 1997. IEEE Standard Specification Format Guide and Test Procedure for Single–Axis Interferometric Fiber Optic Gyros.

IEEE Std. 647, 2006. IEEE Standard Specification Format Guide and Test Procedure for Single-Axis Laser Gyros.

Nassar, S., 2005. Accurate INS/DGPS positioning using INS data de-noising and autoregressive (AR) modeling of inertial sensor errors. *Geomatica*, 59(3), pp. 283-294.

Neumaier A., Schneider T., 2001. Estimation of Parameters and Eigenmodes of Multivariate Autoregressive Models. *ACM Transactions on Mathematical Software*, 27, pp.27- 57.

Savage P. G., 2002. Analytical Modeling of Sensor Quantiza-tion in Strapdown Inertial Navigation Error Equations, *Journal of Guidance, Control, and Dynamics*, 25(5). pp. 833-842.

Schneider T., Neumaier A., 2001. Algorithm 808: ARfit—A Matlab package for the estimation of parameters and eigenmodes of multivariate autoregressive models. *ACM Trans. Math. Softw*. 27(1), pp. 58-65.

Schwarz G., 1978. Estimating the dimension of a model. *Ann. Statis,* 6(2), pp. 461-464.

Zhang X., Mumford P., & Rizos C., 2008. Allan Variance Analysis on Error Characters of MEMS Inertial Sensors for an FPGA-based GPS/INS System. *International Symposium on GPS/GNSS* , November 2008.

Zhao Y., 2011. GPS/IMU integrated system for land vehicle navigation. Licentiate Thesis. Royal Institute of Technology (KTH).
http://kth.diva-portal.org/smash/record.jsf?searchId=1& pid=diva2:446078